Limnol. Oceanogr., 47(5), 2002, 1417–1429

Comparative analysis of energy allocation to tissue and skeletal growth in corals

Kenneth R. N. Anthony,[1] *Sean R. Connolly, and Bette L. Willis*
Department of Marine Biology, James Cook University, Townsville, Queensland 4811, Australia

Abstract

In aquatic invertebrates that form exoskeletons, the partitioning of energy between skeletal and tissue growth is an important tradeoff, especially under resource limitation or physiological stress. Here, we provide the first comparative analysis of energy investment into tissue and skeleton in corals. We develop a mathematical growth model based on colony geometry, tissue mass and quality (enthalpy), and predicted cost of calcification. For hemispherical colonies, the model predicts greater investment in tissue at small sizes, but a shift to skeletal-dominated growth at colony sizes greater than 5–14 cm radius, depending on tissue mass and quality. A similar transition occurs in branches, but is a function of radius and length. An experimental study to assess the impact of resource (light) limitation and physiological stress (sediment load) on energy partitioning in small hemispherical colonies (*Goniastrea retiformis* Lamarck) and branches (*Porites cylindrica* Dana) showed that tissue mass and quality varies greatly over small increments in colony or branch size. In particular, allocations to tissue growth varied tenfold (from positive to negative) more across sediment treatments than did allocations to skeletal growth. A model of energy acquisition versus loss (scope for growth) indicated that tissue growth is more responsive to resource variation and physiological stress than skeletal growth. These results suggest that (1) skeletal and tissue growth rates are weakly correlated across environmental conditions, and that (2) variation in tissue properties is a better proxy for coral health or stress than skeletal growth.

The physiological trade-off of energy allocation is a key life-history trait and the functional basis for maximizing the fitness of organisms (Stearns 1992). Most studies have focused on patterns of energy allocation between growth and reproduction (Tuomi et al. 1983; Kozlowski and Wiegert 1986; Sibly and Calow 1989; Vance 1992) and, more specifically, on the optimal schedule of such allocation (e.g., Chiariello and Roughgarden 1984; Reznick 1990; Perrin and Sibly 1993; Engen and Saether 1994; Shitaka and Hirose 1998; Iwasa 2000). In groups of aquatic invertebrates that produce substantive skeletal structures for support, defense, or protection against environmental extremes (e.g., bivalves, gastropods, corals, bryozoans, echinoids), energy allocation to growth must be further partitioned between skeleton and tissue. Skeletal growth provides the geometric basis for tissue growth and permits organisms to attain a large biomass, which in turn provides the basis for a large reproductive output. The growth of tissue is therefore expected to correlate tightly with that of skeleton, their relative allocations being a function of geometry and size (e.g., Barnes 1973; Hilbish 1986; Middleton et al. 1998; Sebens 1987). In colonial, sessile, invertebrates such as corals and bryozoans, colonies take on geometries ranging from runners and sheets to mounds and trees (Jackson 1979), with tissues often forming a relatively uniform layer over an external skeleton (e.g., Barnes and Lough 1992). Because tissue scales mainly with colony surface area in most coral species (but note that tissue penetrates throughout the skeleton of, for example, acroporids, turbinarians, and fungiids) and skeleton scales mainly with colony volume, relative energy investment in tissue versus skeletal growth will vary with colony size and geometry. This raises two questions. First, to what extent is the relative allocation to tissue and skeleton governed by colony size and geometry? Second, how variable is investment into skeleton and tissue (i.e., in terms of mass and enthalpy) in response to environmental conditions?

One mechanism that could cause deviations from allocation patterns predicted by geometry is that tissue and skeletal growth may not be equally coupled to the physiological energetics of the organism. For example, Hilbish (1986) found that tissue growth and shell growth in mussels (*Mytilus edulis*) show different seasonal patterns, with skeletal growth preceding tissue growth. Also, Barnes and Lough (1999) found that the thickness of the tissue layer in massive colonies of the coral, *Porites* sp., correlated inversely with rates of sedimentation, whereas skeletal growth rates were relatively invariant. Such variation in the responses of tissue and skeletal growth rates will have implications for the growth energetics of corals, although the magnitude of deviations from standard allocation models may depend on an organism's size, growth form, and physiological status. Previous work indicates that many aspects of the physiological ecology of corals vary with colony size and shape (e.g., Barnes 1973; Sebens 1987; Patterson 1992; Kim and Lasker 1998). However, there is currently no theoretical framework within which to formally analyze how patterns of energy allocation between skeletal structures and somatic tissue in calcifying marine invertebrates vary with colony size.

Here, we investigate the relative importance of growth form, size, tissue mass, tissue quality, and skeletal density in predicting patterns of energy allocation, using reef-building corals as a model system. Specifically, we ask three questions: First, how does allometric growth affect energy

[1] Corresponding author (Kenneth.Anthony@jcu.edu.au).

Acknowledgments

This study was funded by the Australian Research Council, CSIRO Marine Division, and CRC Reef Research. We are grateful to Dave Barnes, Michael Lesser, Ken Sebens and an anonymous reviewer for comments that improved the manuscript. This is contribution number 5 from the Centre for Coral Reef Biodiversity at James Cook University.

allocation to tissue and skeleton in the absence of plasticity in response to the environment? Second, how do allocation patterns vary with colony size? Third, how does the allocation pattern to tissue and skeleton vary with energy acquisition and environmental stress? Common reef-building scleractinian corals, such as *Porites* and faviids, are ideal tools for investigating the impacts and interactions between geometry, size, and physiological status on allocation patterns. In these groups, tissues form a layer over a carbonate matrix, and the total tissue mass is thus limited by the rate of expansion of the skeletal surface and vice versa.

To address these questions, we undertook three studies. First, to compare effects of tissue mass, tissue quality, and skeletal density on energy investment patterns as a function of morphology and size, we developed a mathematical growth model based on coral geometry and the bioenergetics of tissue synthesis and calcification. Second, to assess variation in energy allocation patterns in response to environmental stress (and thus partially examine model assumptions and deviations from predictions), we examined patterns of energy allocation for colonies of a hemispherical and a branching coral species subjected to manipulated light and sediment levels in a tank experiment (*see* Anthony 1999*b*). Third, to investigate the trophic basis for patterns of energy allocation to tissue and skeleton under varying resource (light) and stress (sediment) conditions, we analyzed empirical growth data using the model of scope for growth (SfG) defined as the difference between energy acquisition and loss (Warren and Davis 1967; Maltby 1999; *see also* Sebens 1979; Kim and Lasker 1998).

Energy investment models—Total energy invested into growth of a coral colony can be represented as the sum of energy invested in past tissue and skeletal growth:

$$E_{\text{tot}} = E_T + E_S \tag{1}$$

where E_T is energy invested into tissue growth and E_S is energy invested into skeletal growth. Additional energy investment during an interval of growth, then, is simply the change in total energy investment, ΔE_{tot}, associated with a small change in colony size, Δx, where x is some measure of colony size, such as colony radius or branch length. This additional energy investment can be partitioned into its tissue and skeletal growth components:

$$\frac{\Delta E_{\text{tot}}}{\Delta x} = \frac{\Delta E_T}{\Delta x} + \frac{\Delta E_S}{\Delta x} \tag{2}$$

Because coral tissue forms a layer over the volume of skeleton, energy invested in the addition of new tissue during a small change in size, Δx, can be expressed with a first-order Taylor approximation as follows:

$$\frac{\Delta E_T}{\Delta x} = \frac{\partial}{\partial x}\left(\frac{S m_T \xi_T}{c_T}\right) = \left(\frac{m_T \xi_T}{c_T}\right)\frac{\partial S}{\partial x} + S\frac{\partial}{\partial x}\left(\frac{m_T \xi_T}{c_T}\right) \tag{3}$$

where $\partial/\partial x$ represents the derivative with respect to x, S is colony surface area, m_T is area-specific dry tissue mass (i.e., the mass of tissue found per unit area of colony surface), ξ_T is mass-specific energy content (the energy contained per unit dry tissue mass), and c_T is the net metabolic conversion (or production) efficiency (the energy content of tissues relative to the energy invested in tissue production, Withers 1992). The first term on the right-hand side represents the energy cost of adding tissue to cover the increment in surface area associated with growth, and the second term represents any change in the energy content of existing tissue. Similarly, skeletal energy investment over a growth interval can be expressed as

$$\frac{\Delta E_S}{\Delta x} = \frac{\partial}{\partial x}(V \rho_S \xi_S) = \rho_S \xi_S \frac{\partial V}{\partial x} + V\frac{\partial}{\partial x}(\rho_S \xi_S) \tag{4}$$

where V is colony volume, ρ_S is (dry) skeletal density, and ξ_S is the energy cost of calcification per unit dry weight. The first term on the right-hand side represents the energy cost of adding skeleton to fill the increment in colony volume associated with growth, and the second term represents any change in the volume-specific energy cost of calcification. It is important to note that this model is concerned specifically with the additional energy needed by a coral to add the tissue and skeleton for an increase in size, over and above any energy expended in maintenance (e.g., turnover of existing tissue). Thus, it is not, and is not intended to be, a complete energy budget. Rather, Eqs. 3 and 4 characterize how the energy invested in growth is partitioned between tissue and skeleton—both new tissue and skeleton, and changes in the energy content per unit area or volume of existing tissue and skeleton.

Clearly, changes in surface area and volume during growth will vary depending on colony shape. Here, we use standard formulas for two simple geometric forms, hemispheres and cylinders, to approximate the shapes of massive and digitate/branching colonies, respectively. Note that ''colony,'' in the latter case, refers to individual branches. Total colony growth would be obtained by summing energy investment across all branches. During growth, colony radius and/or (for branching forms) branch length may change. Therefore, we characterized the relative magnitudes of tissue and skeletal growth as functions of these variables. We conduct an initial analysis mathematically, in order to determine general properties of these relationships. We then use experimentally derived parameter values to illustrate those properties for massive and branching growth forms.

Assumptions—Given the lack of formal theory of energy allocation to skeletal versus tissue growth in coral colonies, we begin with simple models in which the parameters m_T, ξ_T, c_T, ρ_S, and ξ_S are constants. With these assumptions, the second terms on the right-hand sides of Eqs. 3 and 4 are zero, and the energy cost of growth is dominated by the energy invested in the new tissue and skeleton needed to fill the surface area and volume that are added during a growth interval (the first terms on the right-hand sides of Eqs. 3 and 4). Indirect evidence suggests that these assumptions will be violated to some degree. For instance, the skeletal density (ρ_S) of a species may vary among habitats (Hughes 1987) as well as seasons (e.g., Barnes et al. 1989). Likewise, intraspecific variation in area-specific tissue mass (m_T) can be substantial (as much as twofold), even for similarly sized colonies (Anthony unpubl. data). We identify deviations from these assumptions by comparison of model predictions

Table 1. Parameter values (lower and upper bounds) used to model energy investment in tissue and skeletal energetics as a function of geometry and size. *See text* for the derivation of the parameter for the energetics of calcification.

Parameter	*Goniastrea retiformis*		*Porites cylindrica*		Source
	Lower	Upper	Lower	Upper	
Tissue mass (m_T, mg cm^{-2})*	13.4	18.8	6.4	9.5	Anthony (unpublished), this study
Tissue enthalpy (ξ_T, J mg^{-1})†	25.5	33.3	25.5	33.3	Gnaiger and Bitterlich (1984), Leuzinger (unpubl. data)
Skeletal density (ρ_S, mg cm^{-3})*	1,387	1,491	1,389	1,479	This study
Energetics of calcification (ξ_S, J mg^{-1})	0.152	0.152	0.152	0.152	McConnaghey and Whellan (1996), Anthony and Fabricius (2000)

* Calculated using lipid : protein ratios of 1 : 9 and 6 : 4 for low and high tissue qualities and specific enthalpies of 39.5 J mg^{-1} for lipid and 23.9 J mg^{-1} for protein.
† Lower and upper levels for each parameter are estimated as the mean ±2 SE of 10–15 samples.

with observed patterns of allocation to skeletal and tissue growth of corals under varying environmental conditions (light and sediment concentration, *see Experimental Study*). These deviations can then inform further development of the theory.

Parameters—Upper and lower bounds for the two key tissue (m_T and ξ_T) and skeletal (ρ_S and ξ_S) parameters are presented in Table 1. These values are representative maxima and minima of typical ranges for the massive coral *Goniastrea retiformis* and the branching coral *Porites cylindrica* (Fig. 1). Note, however, that the results of model analyses are not specific to these parameter ranges, and thus should be representative of generalized massive and branching growth forms under the assumptions outlined above.

Tissue parameters: Estimates of mass-specific energy content (ξ_T) were based on the enthalpy of the major tissue constituents: lipid (39.5 J mg^{-1}), protein (23.9 J mg^{-1}), and carbohydrates (17.5 J mg^{-1}, Gnaiger and Bitterlich 1984; Anthony and Fabricius 2000). Recent biochemical data for eight coral species (S. Leuzinger pers. comm.) indicate that carbohydrate content is negligible in coral tissue and that most variation in tissue quality is due to lipids. Since area-specific tissue mass (m_T) depends upon the thickness of the tissue layer, it can be expected to differ between the small-polyped branching and the large-polyped massive species.

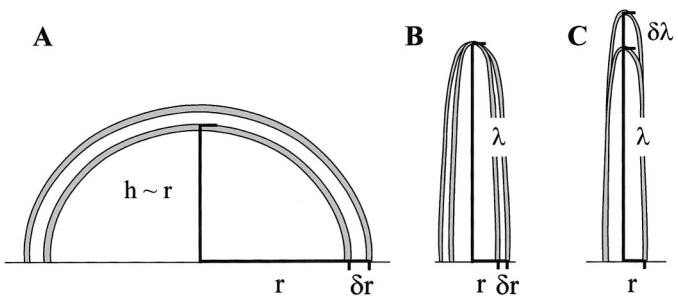

Fig. 1. Longitudinal-section diagrams of tissue and skeletal mass in (A) massive, hemispherical, and (B) and (C) branching (digitate) corals. The shaded area represents the tissue layer. Two scenarios were modeled separately for the digitate morphology: (B) branch thickening and (C) lengthening. The species *Goniastrea retiformis* and *Porites cylindrica* were used as examples.

Experimental work (Anthony unpubl. data) indicates that m_T in *G. retiformis* and *P. cylindrica* may vary from 13.4 to 18.8 mg cm^{-2}, and 6.4 to 9.5 mg cm^{-2}, respectively (Table 1). Very few data exist on metabolic conversion efficiency (c_T) of symbiotic cnidarians. Based on data for other animal groups (Withers 1992; Bayne 2000), we used 75% as a conservative value.

Skeletal parameters: We estimated skeletal density (ρ_S) empirically as the ratio of skeletal dry weight to colony volume using 15 specimens per species, which spanned a common size range (*G. retiformis*: 30–1,200 g; *P. cylindrica*: 5–100 g), to control for effects of colony size on density. Each specimen was first weighed while dry, then soaked for 3 d in fresh water to minimize air in the skeleton, and subsequently weighed while submerged (buoyant weight). Using Archimedes' principle, the difference between dry and buoyant weight provided an estimate of colony density. This protocol yielded estimates of 1.46 ± 0.09 (SD) × 10^3 mg cm^{-3} for *G. retiformis* and 1.42 ± 0.08 × 10^3 mg cm^{-3} for *P. cylindrica* (Table 1), with negligible effects of colony or branch size. Energy cost of calcification (ξ_S) was estimated based on the predicted expenditure of 1 mole of ATP for every 2 moles of Ca^{2+} that are transported across the membrane of calicoblastic cells to the site of calcification (McConnaghey and Whelan 1997; Anthony and Fabricius 2000). Since 1 mole of ATP equates to 30,500 J (Zubay 1983) and 2 moles of $CaCO_3$ equates to 2 × 10^5 mg dry weight, the deposition of 1 mg dry weight of $CaCO_3$ is expected to require 0.152 J. The energy cost of producing organic skeletal matrix was assumed to be negligible based on the results of Allemand et al. (1998).

Hemispherical colonies: Because the size (surface area and volume) of a hemisphere is completely described by its radius (Fig. 1A), growth of a hemispherical coral can be modeled as

$$\frac{\Delta E_T}{\Delta r} = 4\pi r \frac{m_T \xi_T}{c_T} \tag{5}$$

for tissue, and

$$\frac{\Delta E_S}{\Delta r} = 2\pi \rho_S r^2 \xi_S \tag{6}$$

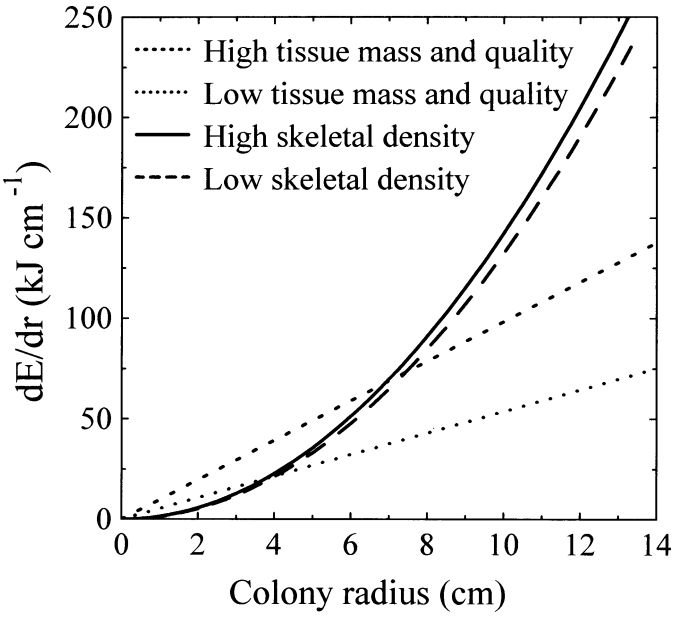

Fig. 2. Hemispherical colonies: Effects of tissue mass and quality, skeletal density, and colony size on energy investment into tissue and skeleton per increment in colony radius (Eqs. 5 and 6). *See Table 1* for parameter values.

for skeleton, where r is colony radius (*see* Web Appendix 1 at http://www.aslo.org/lo/toc/vol_47/issue_5/1417a1.pdf for details). Note that energy invested in tissue growth per growth interval (i.e., per increment of colony radius, δr) increases linearly with colony radius, while energy invested in skeletal growth per increment in radius increases with the square of colony radius. Moreover, these lines will cross. That is, there is a critical colony radius (r_{crit}) for which an increment in colony size requires equal investment into tissue and skeletal growth (*see also* Barnes 1973 for module-surface-volume determinants of critical radius). We can find this by setting Eqs. 5 and 6 equal to one another and solving for r

$$r_{crit} = \frac{2m_T\xi_T}{c_T\rho_S\xi_S} \tag{7}$$

r_{crit} increases as (a) tissue mass and/or quality increases (m_T ξ_T) and (b) energy cost of skeletal growth decreases (ρ_S ξ_S). When $r < r_{crit}$, more energy is allocated to tissue growth; when $r > r_{crit}$, more energy is allocated to skeletal growth.

We illustrate these results using parameter values based on the massive coral *G. retiformis* (Fig. 2). Most notably, $r_{crit} \sim 3.5$ cm for low tissue mass and quality, while $r_{crit} \sim 6.5$ cm for high tissue mass and quality. Variation between minimum and maximum skeletal density caused only minor variation in the location of r_{crit} (<1 cm). Thus, energetic investment into tissue dominates while the coral is still small ($r < 4$–6 cm, depending on tissue mass and quality). As colony size increases beyond r_{crit}, skeletal growth increasingly dominates colony energy investment.

Branches: Growth of a colony branch is a function both of branch radius, r, and of branch length, λ (Fig. 1B). Here, we model the effects of branch thickening and branch lengthening with separate equations. We expect that actual branch growth will approximate ''branch lengthening'' relatively closely, since most branch growth is characterized by increases in length but minimal change in thickness. However, by presenting equations for both thickening and lengthening, branch growth that includes any pattern of relative allocation to lengthening and thickening can be accommodated (*see* Web Appendix 1 for details). We also note that these equations characterize the growth of individual branches. Thus, energy invested in growth for a branching colony is simply the sum of the energy invested in the growth of the individual branches, where each branch will have its own radius and length.

Branch thickening: Changes in tissue and skeletal energy content associated with growth in branch thickness (radius) are

$$\frac{\Delta E_T}{\Delta r} = 2\pi(\lambda + r)\frac{m_T\xi_T}{c_T} \quad \text{and} \tag{8}$$

$$\frac{\Delta E_S}{\Delta r} = 2\pi\xi_S\rho_S\lambda r \tag{9}$$

(*see* Web Appendix 1 for details). Thus, energy invested in new tissue during branch thickening increases linearly with branch length and branch radius, analogous to the allocation pattern predicted for the hemispherical coral. Unlike in the hemispherical model, however, the energy invested in skeleton during branch thickening (Eq. 9) also increases linearly with branch length and branch radius. In other words, the thicker or longer a colony branch is, the greater the cost of an additional increase in radius, but the proportional cost (energy cost relative to branch thickness or length) remains constant.

By setting Eq. 8 equal to Eq. 9 and rearranging, we obtain an expression for the critical branch size at which the costs of additional tissue and skeleton associated with branch thickening are equal. Since the energy allocation equations for branch lengthening include radius and length, the solution to this equation is the set of values (λ, r) that satisfy

$$\frac{\lambda r}{\lambda + r} = \frac{m_T\xi_T}{c_T\rho_S\xi_S} \tag{10}$$

When the left-hand side of Eq. 10 is smaller than the right-hand side, the cost of tissue growth exceeds that of skeletal growth. As with the hemispherical model, this occurs at small sizes (the numerator shrinks faster than the denominator as λ and r approach zero). Conversely, for large enough branches, the cost of adding skeleton exceeds that of tissue during branch thickening (the numerator grows faster than the denominator as λ and r both become large). Two critical sets of length-radius combinations from Eq. 10 are shown in Fig. 3, based on parameter values for *P. cylindrica.* The dotted line corresponds to low tissue mass and quality (lower bounds of tissue mass and enthalpy, Table 1) and mean skeletal density. The dashed line corresponds to the opposite scenario: high tissue mass and quality (and mean skeletal density). Above and to the right of each line,

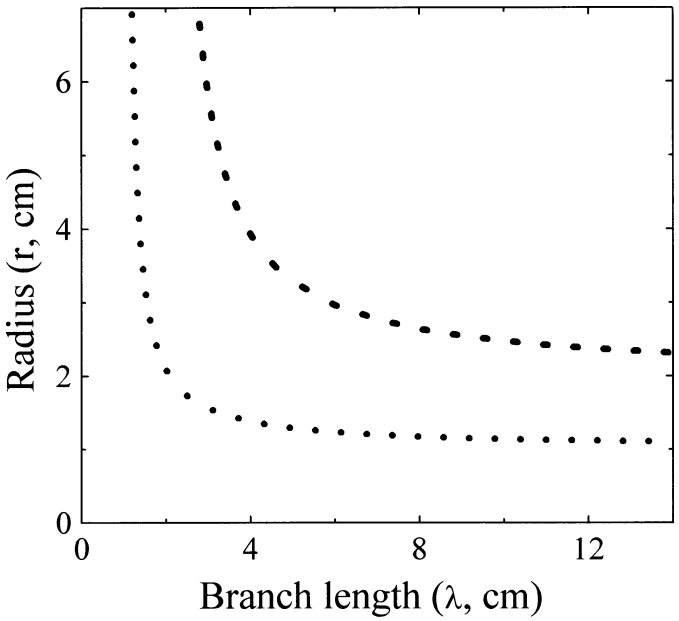

Fig. 3. Curves showing the combinations of branch length and radius for which tissue and skeletal energy investment are equal. Cases are shown for high (dashed line) and low (dotted line) tissue mass and quality, assuming mean skeletal density (*see Table 1*) in both cases. Above and to the right of curves, the addition of skeleton is more costly than the addition of tissue. Below and to the left, tissue is more costly.

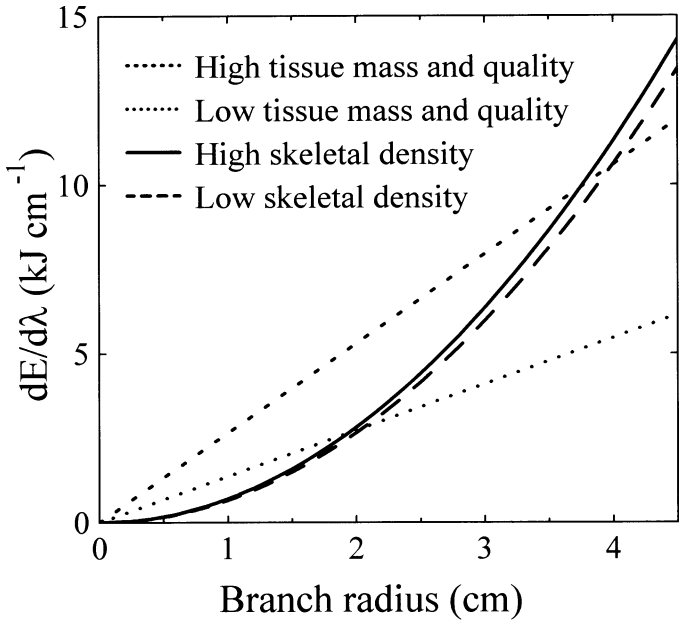

Fig. 4. Branches: Effects of tissue mass and quality, skeletal density, and branch thickness on energy investment into tissue and skeleton per increment in branch length. *See Table 1* for parameter values.

skeletal growth is more costly than tissue growth. Below and to the left of each line, tissue growth is more costly than skeletal growth. For the high tissue-mass/quality parameter set, r goes to infinity as λ approaches approximately 2 cm, and vice versa. Thus, for branch lengths shorter than 2 cm, tissue growth is more costly than skeletal growth regardless of branch radius. This approximates the whole-colony state when it is primarily an encrusting base. Conversely, for branch radii smaller than 2 cm, tissue growth is more costly than skeletal growth regardless of branch length. For the low tissue-mass/quality parameter set, this value is approximately halved to 1 cm.

Branch lengthening: Changes in tissue and skeletal energy content associated with branch lengthening are

$$\frac{\Delta E_T}{\Delta \lambda} = 2\pi r \frac{m_T \xi_T}{c_T} \quad \text{and} \tag{11}$$

$$\frac{\Delta E_S}{\Delta \lambda} = \pi r^2 \rho_S \xi_S \tag{12}$$

(*see* Web Appendix 1 for details). Unlike branch thickening, energy invested in tissue and skeleton during branch lengthening increases with branch radius but not branch length. Because tissue energy investment increases linearly with branch radius, while skeletal investment increases with the square of branch radius, the energetics of branch lengthening are qualitatively identical to those of colony growth in the massive coral. Thus, as with the massive colony, there is a critical branch radius at which the energetic costs of new tissue and new skeleton associated with branch lengthening are equal. This critical radius is given by exactly the same formula for both branching and massive corals (Eq. 7). As in the massive model, when $r < r_{crit}$, the cost of added tissue exceeds that of added skeleton during branch lengthening. Conversely, when $r > r_{crit}$, adding skeleton is more costly.

Again, we illustrate these results using parameter values based on the digitate coral *P. cylindrica* (Fig. 4). At minimum and maximum tissue mass and quality, r_{crit} is approximately 2 or 3.5 cm, respectively. As for the hemispherical model, variation between minimum and maximum skeletal density had only minor influence on the location of r_{crit} (<0.5 cm). Thus, investment in tissue dominates the energetic cost of lengthening for branches with a radius less than 2–4 cm, depending on tissue mass and quality. For thicker branches (approaching massive or columnar morphologies), skeletal growth increasingly dominates the cost of branch lengthening.

Experimental growth study—In the model presented above, the partitioning of energy between tissue and skeletal growth is not affected by either the rate of energy acquisition or the physiological status of the coral. In other words, a stressed coral, which acquires surplus energy at a low rate, would partition energy in the same way as an unstressed coral. It is unlikely that such assumptions are appropriate. For instance, mass-specific energy content (ξ_T) will vary with tissue composition, in particular with the content of lipid, which is a high-energy tissue component (Gnaiger and Bitterlich 1984). To assess the nature of deviations from these model assumptions, we analyzed data on tissue and skeletal growth for small colonies of *G. retiformis* (~2.5 cm radius) and branches of *P. cylindrica* (4.5–6.5 cm length,

Table 2. Growth data for hemispherical (*Goniastrea retiformis*) and digitate (*Porites cylindrica*) before and after 2 months of exposure to manipulated shading and sediment conditions in a tank experiment (*see* Anthony 1999*b* and Anthony and Fabricius 2000). Indices 1 and 2 refer to days 1 and 60. Standard deviations are given in parentheses. *See text* for details of geometric measurements. Estimates of ξ_{T1} and ξ_{T2} are based on the measured proportion of lipids and proteins (by difference) and their specific enthalpies (lipid, 39.5 J mg^{-1}; protein, 23.9 J mg^{-1}). For compactness, field categories are omitted.

Light treatments*	Sediment concentration†	Geometric data						Tissue properties					
		N	r_1 (mm)	r_2 (mm)	λ_1 (mm)	λ_2 (mm)	ΔES (J)	N	m_{T1} (mg cm^{-2})	m_{T2} (mg cm^{-2})	ξ_{T1} (J mg^{-1})	ξ_{T2} (J mg^{-1})	ΔET (J)
G. retiformis													
Shaded	Filt	28	22.7 (3.2)	23.2 (3.2)			379	7	16.4	16.2 (0.5)	33.2	33.3	640
	Raw	28	22.8 (3.1)	23.3 (3.1)			385	6	(1.1)	16.2 (0.7)		33.1	581
	Low	28	23.7 (3.5)	24.2 (3.5)			361	9		16.9 (0.7)		33.6	1606
	High	27	23.6 (3.2)	24.0 (3.2)			372	7		17.7 (1.3)		35.0	3512
Unshaded	Filt	27	24.0 (3.3)	24.7 (3.4)			539	7	16.4	16.8 (0.7)	33.2	34.3	2249
	Raw	28	24.7 (4.1)	25.3 (4.1)			514	7	(1.1)	17.1 (0.3)		34.0	2525
	Low	28	23.3 (3.5)	24.0 (3.5)			492	6		18.0 (0.5)		34.8	4010
	High	28	23.4 (3.9)	23.9 (3.9)			388	8		18.4 (0.3)		35.1	4473
P. cylindrica													
Shaded	Filt	28	5.7 (0.9)	5.9 (1.0)	50.5 (5.2)	54.0 (5.4)	166	6	8.3	7.9 (0.5)	32.0	31.5	171
	Raw	32	5.6 (1.0)	5.8 (1.0)	50.4 (5.8)	52.5 (6.1)	138	7	(0.9)	7.9 (1.9)		32.1	159
	Low	32	5.6 (0.9)	5.9 (0.9)	50.3 (3.6)	54.0 (3.8)	175	5		8.2 (0.4)		31.8	419
	High	20	5.9 (1.1)	6.1 (1.1)	48.4 (3.8)	51.9 (4.0)	155	7		7.6 (0.6)		29.8	−322
Unshaded	Filt	31	6.4 (1.1)	6.7 (1.1)	49.6 (3.8)	53.0 (4.0)	234	9	8.3	7.9 (1.8)	32.0	32.9	532
	Raw	29	5.9 (1.1)	6.2 (1.2)	49.3 (6.6)	51.8 (7.0)	195	5	(0.9)	8.5 (1.0)		34.1	1049
	Low	30	5.7 (0.8)	6.0 (0.8)	49.1 (4.3)	51.6 (4.5)	205	6		9.3 (2.0)		34.2	1642
	High	20	5.7 (1.1)	5.9 (1.1)	47.7 (4.0)	51.0 (4.2)	190	8		7.7 (1.2)		32.2	210

* Light treatments (mol photons m^{-2} d^{-1}): shaded 2.5–2.9, unshaded 9.9–10.7.
† Sediment concentration (mg L^{-1}): filt 0.6–0.9, raw 1.8–2.9, low 3.6–4.4, high 14.4–17.2.

0.5–0.7 cm radius) from the study by Anthony and Fabricius (2000). Colony sizes of *G. retiformis* thus approximated r_{crit} (*see above*), and branch dimensions for *P. cylindrica* satisfied $r < r_{crit}$ and $\lambda < \lambda_{crit}$. Because estimates of tissue parameters (m_T, ξ_T) are associated with relatively large measurement error, the use of small colony sizes, at which relative tissue investment is expected to be high, maximized the precision of these estimates.

Data on colony and branch growth (as linear extensions) and tissue mass and quality (as relative lipid content) were obtained according to a two-factorial design for light level and sediment concentration (Table 2) over a period of 8 weeks using ~250 colonies of *Goniastrea retiformis* and ~300 branches of *Porites cylindrica.* Details of the experimental setup are given in Anthony (1999*b*). Briefly, data on tissue mass (m_T) were obtained as dry weights of decalcified tissues (15–20 colonies or branches) sampled from the natural population prior to experimentation and from within treatment groups at completion of the experiment. Because some organics are likely to be lost during the decalcification process, our estimates of tissue mass should be considered conservative. Tissue energy content (ξ_T) was estimated based on the relative content of lipid (39.5 J mg^{-1}, *see* Anthony and Fabricius 2000 for details of lipid analyses), assuming that nonlipid tissue consisted primarily of protein (23.9 J mg^{-1}). Recent work on the biochemical composition of coral tissues provides support for this assumption (Leuzinger pers. comm.).

The radius of each colony of *G. retiformis* was calculated as the mean of multiple measurements of colony diameter divided by 2. The r of the hemispherical shape approximated by the colony was then obtained as the mean of the height and mean radius (Fig. 1). Although the height was on average approximately 10% smaller than the radius, the bias this introduced in surface area and volume estimates from a hemispherical model was minimal (<5%). Similarly, radii and lengths of *P. cylindrica* branches were obtained from multiple measurements, including measurements at the base and above the middle of each branch.

In addition to measurements of linear extension, skeletal growth was also measured by buoyant weight (w_B) before and after the experiment and then converted to skeletal dry weight (w_S) using the conversion factors $w_S = 1.60\ w_B$ for *G. retiformis* and $w_S = 1.71\ w_B$ for *P. cylindrica* as determined by Anthony (1999*b*). To minimize passive Ca^{2+} exchange, which may affect rates of net calcification (Tambutte et al. 1995), only corals without naked patches of skeleton were used. For *Goniastrea retiformis,* skeletal undersurfaces were all covered by either epoxy putty or encrusting coralline algae. For *Porites cylindrica,* the branch bases were embedded in epoxy putty and the growth of live tissue onto the stands sealed the dead base from the environment, thus preventing passive Ca^{2+} exchange. A summary of the data is presented in Table 2.

Because rates of tissue and skeletal growth are expected to be interrelated, we tested their energetic relationship for each species using principal-axis correlation (Sokal and Rohlf 1995) based on group means (Table 2, data normalized to surface area and expressed as monthly rates). The slopes of the ΔE_S versus ΔE_T curves were calculated from the eigenvalues of the variance–covariance matrices using the method outlined in Sokal and Rohlf (1995).

Table 3. Results of principal-axis correlations for energy investment into skeleton versus tissue (in units of J cm^{-2} $month^{-1}$) determined from among-group as well as within-group variation (*see also Fig. 5*). Also presented are coefficients of variation for tissue and skeletal growth ($CV_{\Delta ET}$ and $CV_{\Delta ES}$) calculated as the ratio of total variance to grand mean.

	slope (SE)	intercept (SE)	R^2	P	$CV_{\Delta ET}$	$CV_{\Delta ES}$
G. retiformis	0.035 (0.009)	3.49 (0.18)	0.63	0.002	0.81	0.22
P. cylindrica	0.029 (0.007)	3.41 (0.16)	0.38	0.060	1.82	0.19

Correlations between observed tissue and skeletal growth—The correlation between energy investment into skeleton and tissue was highly significant for *Goniastrea retiformis* but not significant for *Porites cylindrica* (Table 3). For both species, however, the slope of the ΔE_T-versus-ΔE_S relationship was only 2–4%, indicating that for every 100 J invested into tissue only 2–4 J were invested into skeleton (Fig. 5, Table 3). Note, however, that the low investment into skeleton relative to tissue is, in part, explained by the small colony/branch sizes in accordance with the model (Figs. 2 and 4). Also, the intercept with the ΔE_S-axis was significantly greater than zero for both species (~3.5 J cm^{-2} $month^{-1}$). Skeletal growth rates thus fall within a relatively narrow, positive range across a wide range of environmental conditions, even in situations where rates of tissue growth are zero or negative. Most strikingly, rates of skeletal growth were all positive for *P. cylindrica*, even in treatment categories (shaded/high sediment) for which tissue growth was negative. Coefficients of variation for energy investment into tissue (based on among-group sums of squares) were fourfold to tenfold greater than those for energy investment into skeleton (Table 3).

Deviations from predictions of the geometric model—To analyze the extent to which varying tissue mass and quality produced deviations from the predictions of the geometric energy investment model, we overlaid the observed rates of total energy investment (E_{tot}, Eq. 1) on those predicted by the model (Fig. 6 and 7). Because predicted and observed skeletal growth were both based on linear extensions, deviations from the model were exclusively attributable to tissue growth. Strikingly, observed energy allocations for *Goniastrea retiformis* in most treatments were located well above the upper boundary of the geometric model, indicating that there was a disproportionate shift of energy allocation toward tissue growth. Also, energy allocations for *Porites cylindrica* in four treatments (unshaded/low sediment load, unshaded/raw, unshaded/filt, and shaded/low sediment load) were above the upper model boundary, signifying a similar disproportionate shift to tissue growth. Conversely, observed energy investment for *P. cylindrica* in the shaded/high-sediment treatment was located well below the lower model boundary, which indicates tissue loss. Importantly, these results indicate that even the use of conservative upper and lower extremes for tissue parameters in the geometric model (under the assumption of constant tissue mass and quality) is not sufficient to account for environmentally induced variation in tissue mass and energy content during extensions.

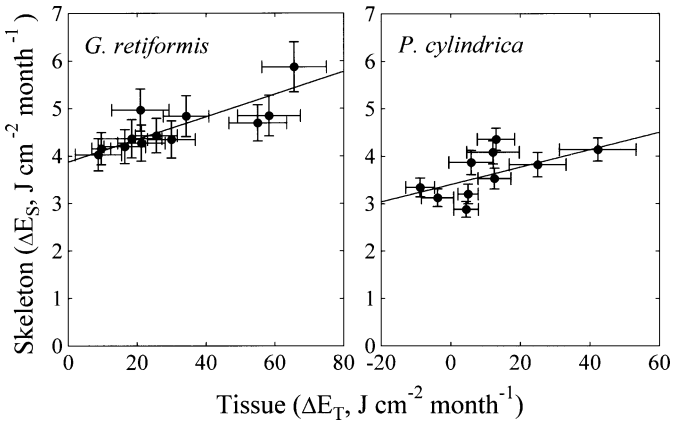

Fig. 5. Principal-axes correlations for energy investment into skeleton (ΔE_S) versus tissue (ΔE_T) during the 2-month growth experiment by Anthony and Fabricius (*see also Table 2*). Data are means ± SE of 16–20 samples. *See Table 3* for results of correlations. Note different *x*-axes.

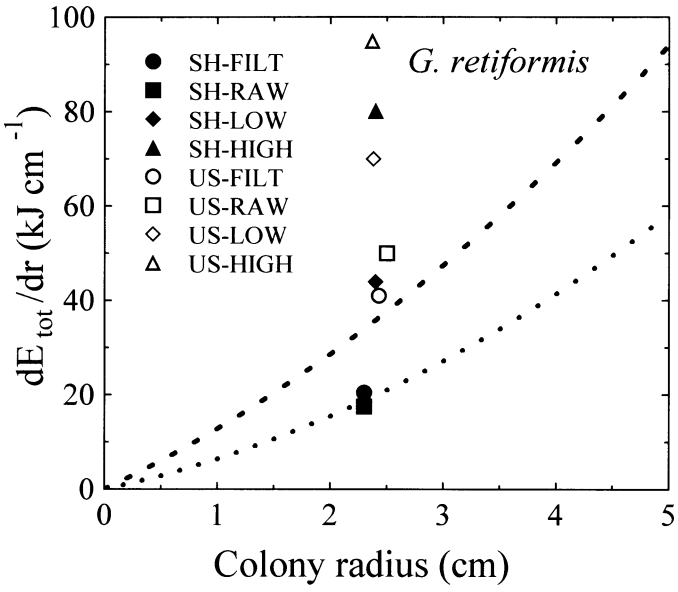

Fig. 6. Rates of total empirical energy investment into tissue and skeleton of *Goniastrea retiformis* under different light and sediment conditions (markers, *see Table 2*) as calculated from increases in colony radius and changes in tissue mass and quality. Lines indicate investment at constant high (dashed line) and constant low (dotted line) tissue masses and qualities as predicted by the geometric model. Mean skeletal density (1,439 mg cm^{-3}, *see Table 1*) was used in the prediction of skeletal investment.

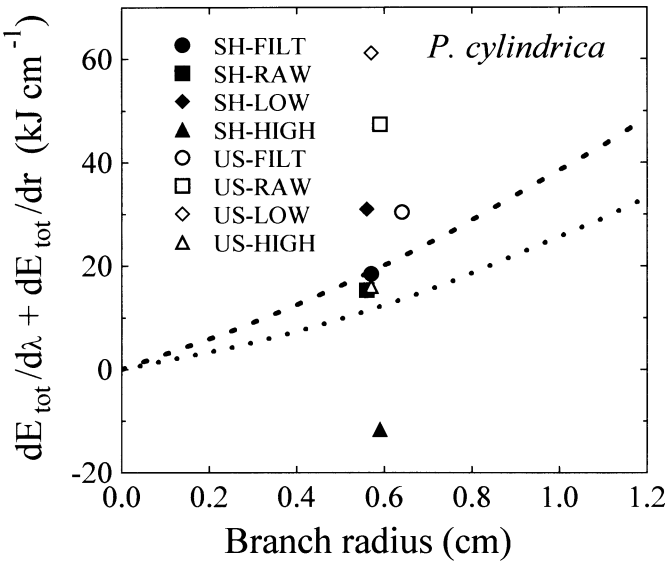

Fig. 7. Rates of total empirical energy investment into tissue and skeleton of *Porites cylindrica* under different light and sediment conditions (markers, *see Table 2*) as calculated from changes in branch dimensions and changes in tissue mass and quality. Lines indicate investment at constant high (dashed line) and constant low (dotted line) tissue masses and qualities as predicted by the geometric model (branch lengthening and thickening). We assumed a constant branch length–radius ratio of 8 based on values in Table 1. Mean skeletal density (1,434 mg cm^{-3}, Table 1) was used in the prediction of skeletal investment.

Energy balance model: physiological predictions of tissue and skeletal growth—To investigate the physiological mechanisms underlying the observed patterns of energy investment and their implications for deviations from geometric predictions, we also analyzed the data using the general model of scope for growth (SfG). SfG is defined as the difference between energy acquisition and that lost via respiration and excretion (Warren and Davis 1967) and is often used as a proxy for organism-level stress or health (Maltby 1999). We parameterized SfG with respect to daily integrated irradiance (I_D) and experimental concentrations of suspended particles (C_{SP}) so that

$$\mathrm{SfG} = P_{(I_D)} + A_{(C_{SP})} - R_{(I_D,C_{SP})} - X_{(I_D,C_{SP})} \qquad (13)$$

where P and A are the predicted daily amounts of energy fixed photosynthetically and heterotrophically (particle feeding), respectively, and R and X are daily respiratory and excretory losses. All terms were expressed in Joules cm^{-2} $month^{-1}$. For simplicity, the unknown terms respiration (R) and excretion (X) were reduced to the term total losses (L), with the assumption that rates of losses above basal metabolism and basal excretion are functions of light level and sediment concentration. However, because the maximum light levels were below those expected to elicit a stress response (<600 μmol quanta m^{-2} s^{-1}), we modeled enhanced losses as a function of sediment concentration only. Also, since only two light levels were used in the experiment, P_{I_D} could be modeled as a linear function of daily integrated light flux. The heterotrophic term ($A_{C_{SP}}$) was modeled using the Michaelis–Menten relationship to account for feeding saturation, particularly in *P. cylindrica* (Anthony 1999*a*). Thus,

$$\mathrm{SfG} = k_1 I_D + \frac{k_2 C_{SP}}{K_M + C_{SP}} - L_B - L_E C_{SP} \qquad (14)$$

k_1 is a coefficient indicating the sensitivity of energy intake to light availability, and k_2 similarly indicates how energy intake varies with increases in particle concentration. L_B is baseline losses, and L_E is a coefficient indicating how rapidly losses increase above baseline as particle concentration increases. K_M is the half-saturation constant in the Michaelis–Menten model, indicating how rapidly energy gain from increasing particle concentration saturates ($K_M \sim 50$ mg L^{-1} for *G. retiformis* and ~3 mg L^{-1} for *P. cylindrica*, Anthony and Fabricius 2000). By fitting Eq. 15 to empirical rates of energy investment into tissue and skeleton, we obtained relative measures of how photosynthesis, feeding, and losses (estimated by k_1, k_2, L_B, and L_E) relate to tissue and skeletal growth across light and sediment regimes.

The SfG model provided a good fit to the empirical energy investments into tissue and skeleton ($R^2 \geq 0.8$ for all data sets; Table 4). In *G. retiformis*, tissue and skeletal growth were both maximized in high-light and high-particle regimes and minimized in low-light and low-particle regimes (Fig. 8), which suggests nutrient limitation at the lowest particle concentrations. In *P. cylindrica*, skeletal growth showed a similar pattern, but tissue growth was maximized at an intermediate particle concentration and minimized at the lowest and highest particle concentrations, the latter indicating sediment stress.

Tissue allocation explained the largest proportion of the variation in particle concentration and light level for both species (Table 4). In *Goniastrea retiformis*, the pattern of tissue energy investment across treatments was predominantly explained by the phototrophic parameter of the model (k_1), which was highly significant. Although *G. retiformis* is an efficient particle feeder, the heterotrophic parameter (k_2) for its tissue energy investment was nonsignificant, in part because the explained variation of the Michaelis–Menten term was compromised by the high saturation constant (Anthony and Fabricius, 2000). The parameters for baseline losses (L_B) and losses enhanced by high particle concentrations (L_E) were nonsignificant in *G. retiformis* (Table 4), the latter indicating relatively little sediment stress within the experimental range. In *Porites cylindrica*, however, both trophic parameters for tissue energetics were significant, but the predicted contribution from heterotrophy was an order of magnitude less than that in *G. retiformis*. Also, the parameter for sediment-enhanced losses was significant in the tissue energetics of *P. cylindrica*, indicating that high-sediment loads within the experimental range caused physiological stress in this species.

In contrast to results for tissue energetics, both of the trophic terms were non-significant for skeletal energetics of *G. retiformis*. In *P. cylindrica*, however, the phototrophic parameter was highly significant, whereas the heterotrophic parameter was nonsignificant. Importantly, the parameters for the trophic terms for both species were 24–35 fold higher for tissue energetics than for skeletal energetics. Also, the

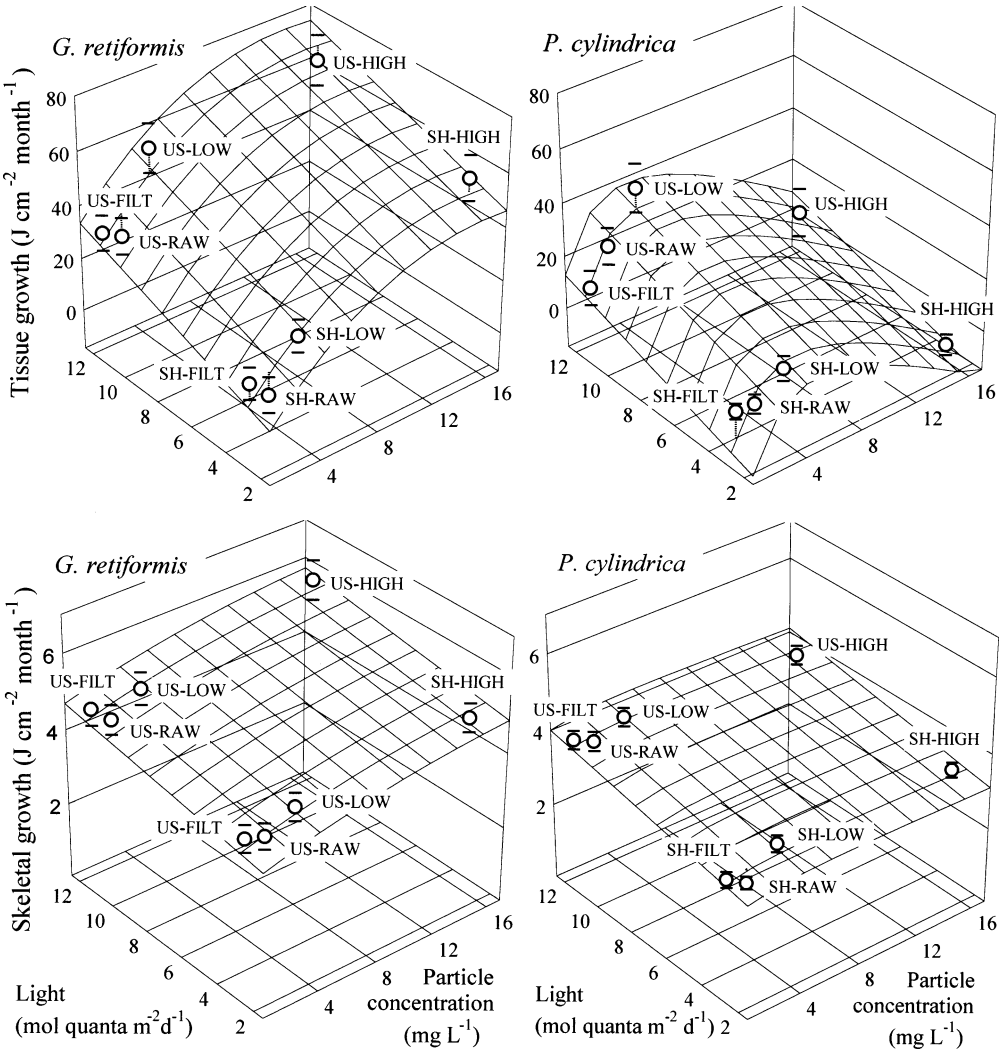

Fig. 8. Nonlinear estimations of the model for SfG fitted to empirical data on energy investment data from Anthony and Fabricius (*see also Fig. 5 and Table 2*). Data are means ± SE of 16–20 samples. *See Table 4* for details of the parameter estimates. The control groups reef slope and reef flat are omitted for clarity.

Table 4. Results of nonlinear estimations of the model of scope for growth (SfG) fitted to the mean rates of energy investment into tissue and skeletal growth (J cm^{-2} month^{-1}). The parameters k_1 and k_2 are coefficients for light (I_D) and particle (c_{SP}) levels to represent phototrophic and heterotrophic contributions, respectively, and L_B and L_E signify baseline losses and losses enhanced by the environmental parameters. *P* values indicate the probability of a given parameter being different from zero.

	G. retiformis			*P. cylindrica*		
	Estimate (SE)	*P*	R^2	Estimate (SE)	*P*	R^2
Total tissue growth						
k_1 (I_D)	2.79 (0.61)	0.006**	0.89	2.23 (0.56)	0.017*	0.90
k_2 (c_{SP})	1,117.61 (527.38)	0.088ns		111.96 (31.97)	0.025*	
L_B (baseline losses)	6.40 (3.75)	0.166ns		18.43 (7.88)	0.079ns	
L_E (enhanced losses)	13.95 (7.93)	0.139ns		5.28 (1.26)	0.014*	
Skeletal growth						
k_1 (I_D)	0.08 (0.03)	0.051ns	0.81	0.09 (0.02)	0.017*	0.80
k_2 (c_{SP})	10.90 (27.68)	0.714ns		0.53 (0.99)	0.619ns	
L_B (baseline losses)	−3.67 (0.35)	<0.001***		−2.80 (0.35)	0.001**	
L_E (enhanced losses)	0.10 (0.41)	0.819ns		0.02 (0.04)	0.692ns	

parameters for the sediment-enhanced losses were 140–314 fold higher in the tissue-energetics compared to the skeletal-energetics model. Most notably, the main descriptors of energy investment into skeleton for both species were the highly negative baseline losses (Table 4), which indicates that a significant amount of energy is invested into skeletal growth despite lack of energy acquisition. Analogously, the nonsignificant coefficients for enhanced losses in the model for skeletal energetics signify that calcification remains relatively invariant across a range of sediment loads. Thus, the model does not predict a stress signal in rates of calcification at high-sediment loads. Overall, these results indicate that the allocation of energy to skeletal growth is less affected by variations in resource availability associated with low light and sediment stress than is the allocation of energy to tissue growth.

Discussion

Linear extension of colony or branch dimensions is one of the most frequently used growth parameters in coral research, in particular in studies of environmental stress (Brown and Howard 1985; Brown et al. 1990; Tomascik 1990; Rice and Hunter 1992; Guzman et al. 1994; Vago et al. 1994; Miller and Cruise 1995; Heiss 1996, earlier studies reviewed by Buddemeier and Kinzie 1976; Brown and Howard 1985). Most research involving coral growth as measured by linear extension, however, has been conducted without the benefit of a formal model for predicting energy investment as a function of size, geometry, and tissue properties. The geometric model presented here, combined with experimental data under a range of environmental conditions, provides a framework for testing whether such linear extensions are a good indication of energy investment, i.e., a proxy for health or stress (e.g., Widdows and Johnson 1988, reviewed by Maltby 1999). Our results indicate that tissue parameters (mass and enthalpy) are far more important than previously assumed and may cause dramatic variations from predictions of a geometric model that assumes tissue constancy during linear extension, in particular for small colony sizes.

Because the ratio of changes in tissue surface area to changes in colony volume scales with $1/r$ in both hemispherical and branching coral, the addition of tissue becomes increasingly constrained with colony or branch size. The geometric model predicted that the growth of hemispherical colonies is tissue-dominated when they are less than 4–7 cm radius, depending on tissue mass and quality. Given that most hemispherical forms grow to several meters in diameter (Veron 1986), one would expect growth to be dominated by allocations to skeleton for the majority of a colony's life. Similarly, the growth of branches greater than 2.0–3.5 cm radius is dominated by allocation to skeleton during linear extension. However, the branch radii of most species are considerably less than 3.5 cm (Veron 1986), so based on our model, we conclude that growth in branching species is generally dominated by allocations to tissue, especially during branch lengthening. Importantly, thin branching morphologies that grow mainly by branch lengthening (e.g., *Porites cylindrica* and most members of the genus *Acropora*) in effect escape the tissue growth limitation of hemispheres and thicker branches (*see also* Barnes 1973).

Deviations from assumptions—The geometric model assumed that tissue parameters (mass per unit area and specific enthalpy) were constants. In other words, the energy content of existing tissue was assumed not to vary over the growth interval, and thus the second term on the right-hand side of Eq. 3 was zero. The experimental data on growth in a range of environmental conditions showed marked deviations from this assumption. Tissue mass and quality varied greatly over small linear extensions, with variation in tissue growth being tenfold that of skeletal growth. Most strikingly, the regression of tissue versus skeletal energy investment in *Porites cylindrica* indicated that positive skeletal growth occurs even when tissue growth is negative. This strongly suggests that variation in the energy content of existing tissue is a major component of the total energetic investment in coral growth, at least for small colonies or branches. Also, because tissue growth depends on the availability of both energy (e.g., through photosynthesis) and nutrients (e.g., though feeding), whereas skeletal growth is mainly driven by photosynthesis (e.g., Barnes and Chalker 1990), differences in the patterns of growth rates of tissue and skeleton across experimental treatments may, in part, be explained by differences in degrees of nutrient availability. Further, these deviations from predictions will potentially be greatest for species with a large dynamic range of tissue qualities (thickness and relative content of lipids). This is illustrated graphically in Fig. 9, in which total energy investment (tissue and skeleton) is plotted for hemispherical corals with low and high tissue mass and quality as a function of radius. (Note that the units on the vertical axis are simply energy, unlike earlier figures showing energy per growth increment.) Two points are notable. First, if a colony has a large tissue mass of high quality, a relatively large linear extension is possible without additional energy investment by a reduction in tissue mass and quality only. This scenario is shown by the arrow labeled *a*. Second, linear extension may underestimate (arrow *b*) or overestimate (arrow *c*) energy investment if tissue mass and quality increases or decreases, respectively. For example, the investment of energy into gonad is possible without linear extension. With increases in colony or branch radius beyond r_{crit}, however, deviations from predictions of a geometric model are expected to decrease, as total tissue mass becomes (quantitatively) less important than total skeletal mass. Because the experimental data presented here used only small colonies and branches ($r < r_{crit}$), for which tissue investment is greater than skeletal investment, they are likely to illustrate an upper margin for such deviations from model predictions.

The large variation in tissue relative to skeletal growth across sediment and light treatments suggests that tissue and skeletal energetics in corals are largely uncoupled, and perhaps even that skeletal growth is maintained at the expense of tissue. We propose that skeletal growth rates are relatively invariant to physiological stress, with tissue either thickening or thinning depending on the remaining resources available for growth. (We note, however, that variation in the concen-

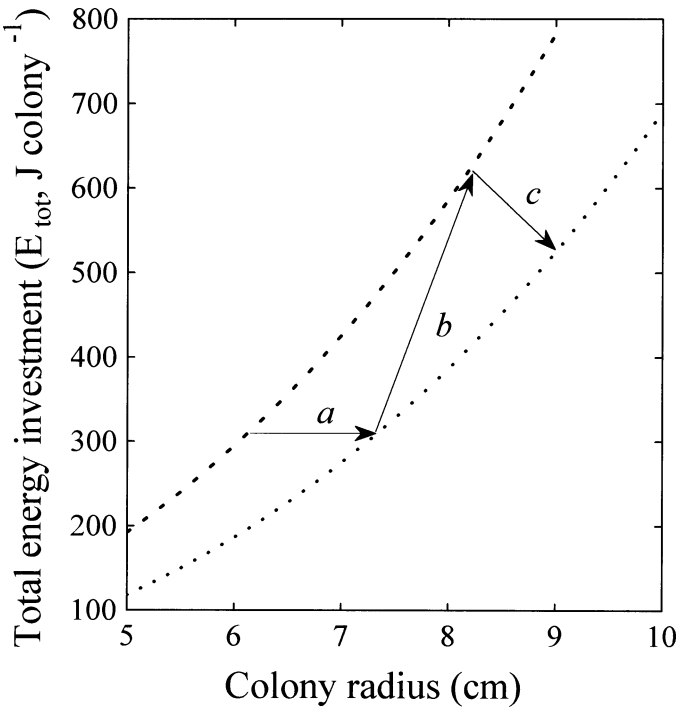

Fig. 9. Possible trajectory of energy investment during three increments in colony radius (linear extension) for a hemispherical coral (*G. retiformis*). Upper (dashed) and lower (dotted) bounds are total (accumulated) investment into tissue and skeleton at high and low tissue masses/qualities, assuming mean skeletal density (Table 1). Variation between curves is thus due to variation in tissue mass and quality only.

tration of inorganic carbon affects skeletal growth rates, e.g., Marubini and Thake 1999.) Under stressful conditions (low light/high sediment) or nutrient limitation (see below), energy and nutrients available for tissues is too limited for tissue growth to keep pace with skeletal growth. As a result, tissue lipids are used to produce the new tissue area necessitated by skeletal growth, and tissue energy content falls. Under benign conditions (high light/low sediment), energy available for tissues exceeds that necessary to keep pace with skeletal growth. Thus, excess energy is stored as lipid, and tissue energy content increases. Such asymmetries between tissue and skeletal growth trajectories under varying environmental conditions have long been known for bivalves (e.g., Hilbish 1986), but have only recently received attention in corals. Barnes and Lough (1999) found that skeletal growth rates of massive *Porites* were relatively invariant along a sediment gradient associated with mining operations, whereas the thickness of the tissue layer correlated inversely with rates of sedimentation.

Energy balance model—The physiological mechanisms underlying such energy partitioning between tissue and skeleton in corals are largely unknown. However, the analysis of the experimental growth data using parameterized functions for heterotrophy, phototrophy, and losses (the model of scope for growth) provides important insight into the effects of resource acquisition and stressors on relative allocations to tissue and skeleton. Our analysis indicates that tissue growth responds more strongly to resource availability and stressors than skeletal growth, which is consistent with our explanation for deviations from the predictions of the geometric model discussed above.

The scope for growth model predicted that energy derived from photosynthesis has a 10–20 fold greater impact on tissue energetics than skeletal energetics. Previous studies have shown that tissues (particularly lipids, Crossland 1987; Harland et al. 1992) and calcification (Barnes and Chalker 1990) are strongly stimulated by photosynthesis. However, the partitioning of energy from photosynthetically fixed carbon to tissues and skeleton has not previously been determined. The greater variation in tissue growth as a function of light and photosynthesis has implications for the use of skeletal growth as a stress parameter given that changes in light regimes are often associated with other potential sources of stress. Perhaps more importantly, the highly negative parameters for baseline losses (L_B) and nonsignificant parameters for sediment-induced losses for skeleton indicated that skeletal investment is highly robust to environmental variation and proceeds at a positive rate under minimum resources and high stress levels.

The pattern of tissue growth in response to light and sediment concentration supports previous suggestions that heterotrophy plays an important role in tissue synthesis, presumably by supplying essential nutrients (Hoegh-Guldberg and Smith 1989; Dubinsky and Jokiel 1994; Muller-Parker et al. 1994) and organic carbon (Anthony 1999*a*). In particular, the striking increase in tissue growth at intermediate (*Porites cylindrica*) or high (*Goniastrea retiformis*) particle concentrations (Fig. 8) clearly indicates the significance of heterotrophy for tissue growth. The role of heterotrophy in skeletal growth is less clear but may indirectly stimulate calcification through tissue growth and by supplying metabolic, inorganic carbon (Furla et al. 2000).

Skeletal energetics—Few attempts have been made to quantify the energy cost of calcification in corals (Falkowski et al. 1984). The results presented here support previous suggestions (Barnes and Chalker 1990) that coral calcification is energetically cheap (signified by a low ξ_S). Given the low predicted value of ξ_S (0.152 J mg^{-1}), skeletal density (ρ_S) has only a minor effect on energy investment during linear extension and could only displace the radius at which tissue energy equals skeletal investment by <1 cm in *G. retiformis*.

Our calculation of energy investment into skeleton is based on the model that Ca^{2+} ions are actively transported across the calicoblastic membrane and into the site of skeletogenesis in exchange for protons in a fixed ratio. The mechanics of this system are now well established (e.g., Barnes and Chalker 1990; Ip et al. 1991; Tambutte et al. 1996), but they have not previously been used for estimating skeletal energetics in corals (but see Anthony and Fabricius 2000). Based on the expected molar ratio of 1 : 2 for ATP and Ca^{2+} involved in the Ca^{2+}/H^+ transport across membranes of calcifying invertebrates (McConnaghey and Whelan 1997), Anthony and Fabricius (2000) calculated that the energy cost of Ca^{2+} exchange in corals translates to 0.152 Joules per milligram of $CaCO_3$ deposited. Two factors can bias such

calculations of skeletal growth energetics: (1) passive Ca^{+2} ion exchange by dissolution of naked skeleton (Barnes and Crossland 1977; Tambutte et al. 1995), and (2) the production of organic matrix (Young et al. 1971; Allemand et al. 1998). The first source of bias was minimized in this study because only corals with an intact tissue surface were used. The second potential source of bias is also considered minimal because Allemand et al. (1998) found that only one mole of aspartic acid (a major constituent of organic-matrix proteins in corals) is incorporated into the organic matrix for every 3.8×10^6 moles of Ca^{2+} incorporated into the skeleton. Assuming, conservatively, that aspartic acid constitutes only 10% of the organic matrix, energy investment into the organic matrix is three orders of magnitude less than the energy cost of active Ca^{2+}/H^+ transport.

In conclusion, the geometric model predicts that the growth of hemispherical corals is tissue dominated at radii less than 4–7 cm but strongly dominated by skeletal growth at radii greater than this, with the transition point increasing with tissue mass and quality. Branches with predominantly apical growth (branch lengthening) are tissue dominated at radii less than 2–4 cm, again depending on tissue mass and quality. The model therefore predicts that the growth of most branching corals ($r < 0.5$–2 cm) is tissue dominated. Energy partitioning will be even more biased toward tissue growth for corals in which tissue is not restricted to a surface layer, for example in species of the common genus, *Acropora.*

The experimental data showed that investment into tissue growth varied fourfold to tenfold more over environmental ranges than did investment into skeletal growth in small colonies (2–3 cm radius) and branches. This variation in tissue growth was greater than predicted by the geometric model, which assumes a constant mass and energy content of existing tissue during colony extensions. Incorporating changes in the mass and quality of existing tissue, including allocation to reproductive tissue, during growth should be a priority for further developments of the model presented here.

Differences between the geometric model and the experimental energetics data suggest that tissue growth is more sensitive to variation in environmental conditions than skeletal growth and that this sensitivity is mediated by changes in tissue mass and quality. The results of the scope for growth modeling support this conclusion: light and sediment load have much larger effects on tissue growth than on skeletal growth.

References

ALLEMAND, D., E. TAMBUTTE, J.-P. GIRARD, AND J. JAUBERT. 1998. Organic matrix synthesis in the scleractinian coral *Stylophora pistillata:* Role in biomineralization and potential target of the organotin tributyltin. J. Exp. Biol. **201:** 2001–2009.

ANTHONY, K. R. N. 1999*a.* Coral suspension feeding on fine particulate matter. J. Exp. Mar. Biol. Ecol. **232:** 85–106.

———. 1999*b.* A tank system for studying benthic aquatic organisms at predictable levels of turbidity and sedimentation: Case study examining coral growth. Limnol. Oceanogr. **44:** 1415–1422.

———, AND K. E. FABRICIUS. 2000. Shifting roles of heterotrophy and autotrophy in coral energetics under varying turbidity. J. Exp. Mar. Biol. Ecol. **252:** 221–253.

BARNES, D. J. 1973. Growth in colonial scleractinians. Bull. Mar. Sci. **23:** 280–298.

———, AND B. E. CHALKER. 1990. Calcification and photosynthesis in reef-building corals and algae, p. 109–131. *In* Z. Dubinsky [ed.], Ecosystems of the world: Coral reefs. Elsevier.

———, AND C. J. CROSSLAND. 1977. Coral calcification: Sources of error in radioisotope techniques. Mar. Biol. **42:** 119–129.

———, AND J. M. LOUGH. 1992. Systematic variations in the depth of skeleton occupied by coral tissues in massive colonies of *Porites* from the Great Barrier Reef. J. Exp. Mar. Biol. Ecol. **159:** 113–128.

———, AND ———. 1999. *Porites* growth characteristics in a changed environment: Misima Island, Papua New Guinea. Coral Reefs **18:** 213–218.

———, ———, AND B. J. TOBIN. 1989. Density measurements and the interpretation of X-radiographic images of slices of skeleton from the colonial hard coral *Porites.* J. Exp. Mar. Biol. Ecol. **131:** 45–60.

BAYNE, B. L. 2000. Relations between variable rates of growth, metabolic costs and growth efficiencies in individual Sydney rock oysters (*Saccostrea commercialis*). J. Exp. Mar. Biol. Ecol. **251:** 185–203.

BROWN, B. E., AND L. S. HOWARD. 1985. Assessing the effects of ''stress'' on reef corals. Adv. Mar. Biol. **22:** 1–63.

———, M. D. A. LE TISSIER, T. P. SCOFFIN, AND A. W. TUDHOPE. 1990. Evaluation of the environmental impact of dredging on intertidal coral reefs at Ko Phuket, Thailand, using ecological and physiological parameters. Mar. Ecol. Prog. Ser. **65:** 273–281.

BUDDEMEIER, R. W., AND R. A. KINZIE. 1976. Coral growth. Oceanogr. Mar. Biol. Annu. Rev. **14:** 183–225.

CHIARIELLO, N., AND J. ROUGHGARDEN. 1984. Storage allocation in seasonal races of an annual plant: Optimal versus actual allocation. Ecology **65:** 1290–1301.

CROSSLAND, C. J. 1987. In situ release of mucus and DOC-lipid from the coral *Acropora variabilis* and *Stylophora pistillata.* Coral Reefs **6:** 35–42.

DUBINSKY, Z., AND P. L. JOKIEL. 1994. Ratio of energy and nutrient fluxes regulates symbiosis between zooxanthellae and corals. Pac. Sci. **48:** 313–324.

ENGEN, S., AND B. E. SAETHER. 1994. Optimal allocation of resources to growth and reproduction. Theor. Pop. Biol. **46:** 232–248.

FALKOWSKI, P. G., Z. DUBINSKY, L. MUSCATINE, AND J. PORTER. 1984. Light and the bioenergetics of a symbiotic coral. Bioscience **34:** 705–709.

FURLA, P., I. GALGANI, I. DURAND, AND D. ALLEMAND. 2000. Sources and mechanisms of inorganic carbon transport for coral calcification and photosynthesis. J. Exp. Biol. **203:** 3445–3457.

GNAIGER, E., AND G. BITTERLICH. 1984. Proximate biochemical composition and calorific content calculated from elemental CHN analysis: A stochiometric concept. Oecologia **62:** 289–298.

GUZMAN, H. M., K. A. BURNS, AND J. B. C. JACKSON. 1994. Injury, regeneration and growth of Caribbean reef corals after a major oil spill in Panama. Mar. Ecol. Prog. Ser. **105:** 231–241.

HARLAND, A. D., P. SPENCER DAVIES, AND L. M. FIXTER. 1992. Lipid content of some Caribbean corals in relation to depth and light. Mar. Biol. **113:** 357–361.

HEISS, G. A. 1996. Annual band width variation in Porites sp. from Aqaba, Gulf of Aqaba, Red Sea. Bull. Mar. Sci. **59:** 393–403.

HILBISH, T. 1986. Growth trajectories of shell and soft tissue in bivalves: Seasonal variation in *Mytilus edulis* L. J. Exp. Mar. Biol. Ecol. **96:** 103–113.

HOEGH-GULDBERG, O., AND G. J. SMITH. 1989. Influence of the

population density of zooxanthellae and supply of ammonium on the biomass and metabolic characteristics of the reef corals *Seriatopora hystrix* and *Stylophora pistillata.* Mar. Ecol. Prog. Ser. **57:** 173–186.

HUGHES, T. P. 1987. Skeletal density and growth form of corals. Mar. Ecol. Prog. Ser. **35:** 259–266.

IP, Y. K., A. L. L. LIM, AND R. W. LIM. 1991. Some properties of calcium-activated adenosine triphosphatase from the hermatypic coral *Galaxea fascicularis.* Mar. Biol. **111:** 191–197.

IWASA, Y. 2000. Dynamic optimization of plant growth. Evol. Ecol. Res. **2:** 437–455.

JACKSON, J. B. C. 1979. Morphological strategies of sessile animals, p. 499–555. *In* B. R. Rosen and G. Larwood [eds.], Biology and systematics of colonial organisms. Academic.

KIM, K., AND H. R. LASKER. 1998. Allometry of resource capture in colonial cnidarians and constraints on modular growth. Funct. Ecol. **12:** 646–654.

KOZLOWSKI, J., AND R. G. WIEGERT. 1986. Optimal allocation of energy to growth and reproduction. Theor. Pop. Biol. **29:** 16–37.

MALTBY, L. 1999. Studying stress: The importance of organism-level responses. Ecol. Appl. **9:** 431–440.

MARUBINI, F., AND B. THAKE. 1999. Bicarbonate addition promotes coral growth. Limnol. Oceanogr. **44:** 716–720.

MCCONNAGHEY, T. A., AND J. F. WHELAN. 1997. Calcification generates protons for nutrient and bicarbonate uptake. Earth Sci. Rev. **967:** 95–117.

MIDDLETON, D. A. J., W. S. C. GURNEY, AND J. D. GAGE. 1998. Growth and energy allocation in the deep-sea urchin *Echinus affinis.* Biol. J. Linn. Soc. **64:** 315–336.

MILLER, R. L., AND J. F. CRUISE. 1995. Effects of suspended sediments on coral growth—evidence from remote sensing and hydrologic modeling. Remote Sens. Environ. **53:** 177–187.

MULLER-PARKER, G., L. R. MCCLOSKEY, O. HOEGH-GULDBERG, AND P. J. MCAULEY. 1994. Effect of ammonium enrichment on animal and algal biomass of the coral *Pocillopora damicornis.* Pac. Sci. **48:** 273–283.

PATTERSON, M. R. 1992. A mass transfer explanation of metabolic scaling relations in some aquatic invertebrates and algae. Science **255:** 1421–1423.

PERRIN, N., AND R. M. SIBLY. 1993. Dynamic models of energy allocation and investment. Annu. Rev. Ecol. Syst. **24:** 379–410.

REZNICK, D. N. 1990. Plasticity in age and size at maturity in male guppies (*Poecilla reticulata*): An experimental evaluation of alternative models of development. J. Evol. Dev. **3:** 185–204.

RICE, S. A., AND C. L. HUNTER. 1992. Effects of suspended sediment and burial on scleractinian corals from West Central Florida patch reefs. Bull. Mar. Sci. **51:** 429–442.

SEBENS, K. P. 1979. The energetics of asexual reproduction and colony formation in benthic marine invertebrates. Am. Zool. **19:** 683–697.

———. 1987. The ecology of indeterminate growth in animals. Annu. Rev. Ecol. Syst. **18:** 371–407.

SHITAKA, Y., AND T. HIROSE. 1998. Effects of shift in flowering time on the reproductive output of *Xanthium canadense* in a seasonal environment. Oecologia **114:** 361–367.

SIBLY, R. M., AND P. CALOW. 1989. A life-history theory of responses to stress. Biol. J. Linn. Soc. **37:** 101–116.

SOKAL, R. R., AND F. J. ROHLF. 1995. Biometry, 3rd ed. Freeman.

STEARNS, S. C. 1992. The evolution of life histories. Oxford Univ. Press.

TAMBUTTE, E., D. ALLEMAND, I. BOURGE, J. P. GATTUSO, AND J. JAUBERT. 1995. An improved ^{45}Ca protocol for investigating physiological mechanisms in coral calcification. Mar. Biol. **122:** 453–459.

TAMBUTTE, R., D. ALLEMAND, E. MUELLER, AND J. JAUBERT. 1996. A compartmental approach to the mechanism of calcification in hermatypic corals. J. Exp. Biol. **199:** 1029–1041.

TOMASCIK, T. 1990. Growth rates of two morphotypes of *Montastrea annularis* along a eutrophication gradient, Barbados, West Indies. Mar. Pollut. Bull. **21:** 376–381.

TUOMI, J., T. HAKALA, AND E. HAUKIOJA. 1983. Alternative concepts of reproductive effort, costs of reproduction, and selection in life-history evolution. Am. Zool. **23:** 25–34.

VAGO, R., E. VAGO, Y. ACHITUV, M. BENZION, AND Z. DUBINSKY. 1994. A non-destructive method for monitoring coral growth affected by anthropogenic and natural long term changes. Bull. Mar. Sci. **55:** 126–132.

VANCE, R. R. 1992. Optimal somatic growth and reproduction in a limited, constant environment—the general case. J. Theor. Biol. **157:** 51–70.

VERON, J. E. N. 1986. Corals of Australia and the Indo-Pacific, 2nd ed. Univ. Hawaii Press.

WARREN, C. E., AND G. E. DAVIS. 1967. Laboratory studies on the feeding, bioenergetics and growth of fish, p. 175–214. *In* S. D. Gerking [ed.], The biological basis for freshwater fish production. Blackwell Scientific.

WIDDOWS, J., AND D. JOHNSON. 1988. Physiological energetics of *Mytilus edulis:* Scope for growth. Mar. Ecol. Prog. Ser. **46:** 113–121.

WITHERS, P. C. 1992. Comparative animal physiology. Saunders College Publishing.

YOUNG, S. D., J. D. O'CONNOR, AND L. MUSCATINE. 1971. Organic material from scleractinian coral skeletons. II. Incorporation of ^{14}C into protein, chitin and lipid. Comp. Biochem. Physiol. B **40:** 945–958.

ZUBAY, G. 1983. Biochemistry, 2nd ed. Addison-Wesley.

Received: 4 September 2001
Accepted: 13 March 2002
Amended: 17 April 2002